International Journal of Hydrogen Energy 58 (2024) 389–399

Contents lists available at ScienceDirect

International Journal of Hydrogen Energy

journal homepage: www.elsevier.com/locate/he

# Effect of high-pressure hydrogen environment on the physical and mechanical properties of elastomers

Geraldine Theiler [a,*], Natalia Cano Murillo [a], Karabi Halder [a], Winoj Balasooriya [b], Andreas Hausberger [b], Andreas Kaiser [c]

[a] Bundesanstalt für Materialforschung und -prüfung (BAM), 12203, Berlin, Germany
[b] Polymer Competence Centre Leoben GmbH (PCCL), 8700, Leoben, Austria
[c] Arlanxeo Deutschland GmbH, Dormagen, Germany

ARTICLE INFO

Handling Editor: Prof I Tolj

ABSTRACT

The development of an infrastructure for the safe and reliable storage, handling and delivery of hydrogen is crucial for the expansion of hydrogen technology in the transport and industrial sector. Since many polymeric materials are directly in contact with hydrogen, it is necessary to conduct further research to study their compatibility with hydrogen. With the increasing demand in material testing in hydrogen, new test facilities are now available at BAM. As a part of the Polymers4Hydrogen project, this study presents the influence of high-pressure hydrogen environment on the physical and mechanical properties of two types of cross-linked hydrogenated acrylonitrile butadiene rubbers. Based on the CSA/ANSI standard, static exposures in hydrogen were performed up to 100 MPa at 120 °C. Characterization before and after exposure was conducted by means of density and hardness measurements, dynamic mechanical analysis (DMA), tensile tests, compression set, FT-IR and AFM analyses to assess effects after decompression. While the effect of high-pressure exposure is significant immediately after exposure, most of the physical and mechanical properties recover after 48 h. FT-IR, AFM, SEM and compression set results indicate, however, permanent effects.

## 1. Introduction

The alarming impact on the environment in the form of global warming, pollution, acid rains, etc. Caused by the exploitation of fossil fuels has made the search for energy efficient carriers even more compelling. The high weather dependency of most of the renewable energy sources (solar, wind, hydro, geothermal, etc.) together with its inherent fluctuations leads to serious supply-demand mismatch problems [1]. This drives hydrogen to be an important energy storage vector for both mobile applications as well as stationary power supplies [2,3]. Hydrogen as an abundantly available energy source with zero pollution has received significant recognition as an important sustainable energy source in the 21st energy century from various countries [4]. Owing to its unique advantages of low energy consumption for compressed hydrogen production, fast charging/discharging rate, etc. [5], great commercial application prospects of hydrogen have already emerged in the energy sector, for example, in fuel cell vehicles (FCVs) and hydrogen fuel stations (HFSs) [6–8]. Furthermore, the recent advancements in the development of hydrogen storage technology, efficient ways of generating green hydrogen and the reduced cost of delivery of hydrogen to the end user, demonstrate every potential of this fuel to become the mainstream energy carrier in the coming decades [9].

However, for the effective usage of hydrogen, it is necessary to ensure the safety and durability of materials exposed to prolonged durations of high-pressure hydrogen environments. Therefore, overcoming the technological challenges and finding the appropriate material compatibility are the prime requisites for the expansion of hydrogen in the transport and industrial sector. To regulate the distribution of high-pressure hydrogen to the FCV, the HFS is equipped with several devices such as accumulator, valves, nozzles, compressor, filters and pre-coolers [10,11]. Nishimura et al. [12] found that a good sealing component, able to reach high-pressure ranges of high storage facilities is one of the primary technical requirements for the connection of all these devices. Elastomeric materials, specifically rubber O-rings have originally been studied as sealing components, however the occurrence of blister fracture during sudden pressure release, limited its wide-scale application

* Corresponding author.
*E-mail address:* Geraldine.Theiler@bam.de (G. Theiler).

https://doi.org/10.1016/j.ijhydene.2024.01.148
Received 28 June 2023; Received in revised form 8 December 2023; Accepted 13 January 2024
Available online 23 January 2024

[13]. Later, the influence of carbon black (CB) and silica on ethylene propylene diene monomer rubber (EPDM) and nitrile butadiene rubber (NBR) composites were studied [14]. While, on one hand, the blister damage with the silica additives was least pronounced, the addition of carbon black raised the hydrogen content of the composite. In yet another study by Nishimura's group [15], the cyclic high-pressure hydrogen exposure on different filled NBR composites indicated that instead of a change in chemical structure, the possible physical degradation (breakage of filler agglomeration and filler-polymer interaction) is attributed to the degradation of the composite material. A reduction of the elastic storage modulus in rubbery state in dynamic mechanical analysis confirmed this phenomenon.

Besides, the experimental work, the performance of rubber O-rings has also been estimated based on some simulation approaches. A finite element model composed of NBR-O rings alone as well as combined with thermoplastic poly(etheretherketone) (PEEK) was built to study this sealing capacity [16,17]. However, until now the preliminary experiments on high-pressure hydrogen exposure were performed only on some common commercial rubber materials such as NBR, EPDM, Viton A and rubber materials with fillers (e.g. silica, carbon black) [14,18]. Characterization of the polymers before and after hydrogen exposure showed a relationship of polymer behavior in hydrogen to polymer microstructure [18]. While the additive incorporated rubbers showed voids around fillers after 90 MPa static hydrogen exposure, long propagating cracks reaching out to the outer surface were found for the Viton-A elastomer. The use of other high-performance or crosslinked elastomers as sealant materials is not prevalent currently, probably due to the lack of sufficient research on their advanced mechanical properties.

This study presents the influence of high-pressure hydrogen environment (static exposure up to 100 MPa) on the physical and mechanical properties of two types of cross-linked hydrogenated acrylonitrile butadiene rubbers (HNBR1 and HNBR2). The state-of-the-art high-pressure hydrogen facility at BAM is exploited in this study. The time of exposure is varied from a period of 7–21 days to consider the aging behavior in long-term hydrogen environments. The changes in exposed specimens such as the dimensions, density, glass transition temperature ($T_g$), tensile properties, compression set properties as well as FT-IR and AFM form the core areas in this paper. A comparison is also made in nitrogen to assess solely the influence of temperature on the properties of the two elastomers. This study will assist in understanding the physical and mechanical properties of two types of elastomers, which are developed for high-pressure gas conditions, and therefore contribute to the selection and development of a high-performance sealing component for the potential hydrogen infrastructure.

## 2. Experimental

### 2.1. Materials

Two different types of crossed-linked elastomers of known grades were provided by Arlanxeo Deutschland GmbH and used for the static hydrogen exposure tests. Both are filled with CB in different compositions and acrylonitrile (ACN) content is relatively low, 21 %, to keep a low glass transition temperature (Tg) and to have good low temperature properties. Additionally, HNBR2 includes Polyamide 6 (here referred as PA) in order to increase the mechanical and thermal properties of the rubber. As described in Ref. [19], the HNBR/PA compounds were prepared by melting at a temperature above the melting point of PA6, which is 221 °C. After dilution with CB, process oil and other compounding ingredients, crosslinking agent were added. The composition and properties of these two rubber materials are listed in Table 1.

The specimen sizes varied in dimensions depending on the test method, except for their thickness which was kept constant at 2 mm (Fig. 1). Following the guidelines for the test methods for evaluating material compatibility in compressed hydrogen applications as outlined in the National Standards of Canada, the elastomers were exposed to dry heat at 60 °C for 48 h before testing [20]. This step is an essential pre-conditioning step for the removal of moisture content and outgassing of the samples that otherwise might have affected the properties of the hydrogen exposed samples.

**Table 1**
Composition and properties of the investigated HNBR.

| | Composition | | | Properties | |
|---|---|---|---|---|---|
| | CB N 550 (phr) | ACN content (%) | PA (phr) | Hardness (ShA) | M100[a] (MPa) |
| HNBR1 | 75 | 21 | – | 79 | 16.5 |
| HNBR2 | 67 | 21 | 10 | 82 | 19.9 |

[a] According to manufacturer data sheet.

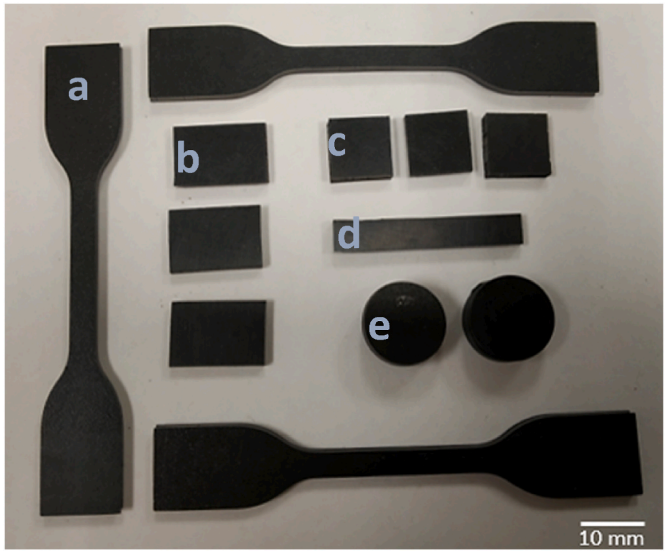


**Fig. 1.** Polymer specimens tested for the hydrogen experiments. a. Specimen for Tensile Test b. Specimen for mass measurement c. specimens for density measurement. d. DMA specimen e. Compression set specimen.

### 2.2. Test methods

#### 2.2.1. High pressure hydrogen testing facility

Static exposures in hydrogen were performed in the hydrogen test facility described in Fig. 2. The HNBR1 and HNBR2 elastomers with varying dimensions were tested according to CSA/ANSI CHMC 2:19 Standard. A set of preliminary tests were initially conducted with three different low-pressure hydrogen exposure conditions: (i) 5 MPa, 85 °C, (ii) 20 MPa, 85 °C and (iii) 20 MPa, 120 °C for a period of 21 days. The study further involved static exposure of the elastomers to high-pressure hydrogen environment using 99.9 % of $H_2$ gas with pressures up to 100 MPa in a sealed chamber at 120 °C for a period of 7 and 21 days.

After being prepared, the samples were introduced first into a glass sample holder and then to the stainless-steel autoclaves (180 mm in length and 18 mm in diameter) inside the autoclave. The system was then held isostatic for 16 h to ensure that an equilibrium hydrogen concentration along with the desired temperature and pressure have been reached. A day before the end of the exposure period the temperature was switched off first, to cool down the specimens before taking them out. A second filling was necessary to replenish the pressure loss due to the cooling effect. The high-pressure hydrogen gas was released on the final day at a very fast rate (<5sec) and the specimens were immediately taken out for further characterization tests. Fig. SM1 in the supplementary material illustrates an example of pressure and temperature progression during a 21 days-experiment. To exclude the influence

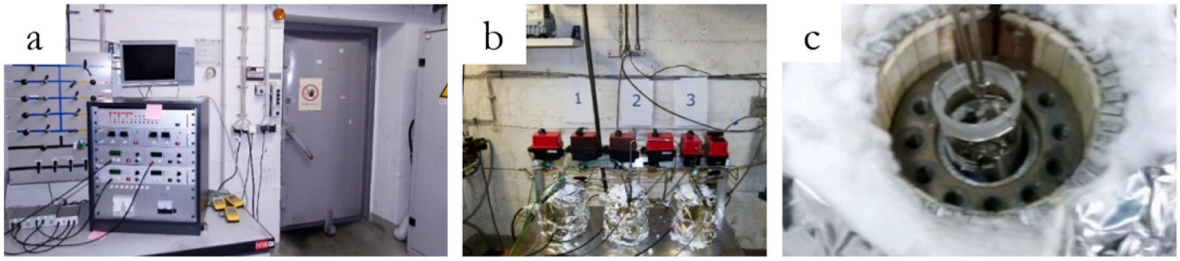


**Fig. 2.** Hydrogen test facility at BAM under static exposure conditions up to 100 MPa, 120 °C for 7 and 21 days. (a) Control room, (b) hydrogen autoclaves, (c) sample container.

of the temperature, control tests were performed in nitrogen atmosphere at 0.1 MPa, 120 °C and for a period of 7 days.

*2.2.2. Characterization tests*

At least three HNBR1 and HNBR2 samples per exposure conditions were used for the characterization tests. The physical characterization tests (mass, dimensions, density) and mechanical tests (dynamic mechanic analysis, tensile, hardness, and compression set) were measured before, immediately after and 48 h after hydrogen exposure. For each of the tests, the control tests in nitrogen atmosphere were also conducted. Regarding the tests immediately after hydrogen exposure, the physical tests were performed within 10 min and the mechanical tests within half an hour after taking out from the hydrogen chamber.

*2.2.2.1. Mass.* The mass of the samples before, immediately after and 48 h after hydrogen exposure was measured using an electronic analytical balance ME235S (Sartorius, Germany). For each of the conditions, an average of three samples were tested for accuracy and reproducibility.

*2.2.2.2. Appearance and dimension.* The optical images and the dimensions of the samples before, immediately after and 48 h after hydrogen exposure were conducted using a VHX-5000 optical microscope (Keyence, Germany). Three sample specimens with a dimension of 15 × 10*2 $mm^3$ were tested for each of the exposure conditions. The images recorded had a lateral resolution of 1 μm and a vertical resolution of 0.1 μm. For each of the conditions, a panorama image with a magnification of 50× and a magnified image with a 100× magnification was recorded. Furthermore, AFM analyses were performed on selected samples with an Asylum Research Cypher microscope.

*2.2.2.3. Density.* Density measurements for both the elastomers were performed gravimetrically using the method as described in the ISO 1183-1 standard. The specimen densities were measured before, immediately after and 48 h after taking out from the hydrogen chamber on samples with a dimension of 10 × 10*2 $mm^3$. The mass of the samples in air were determined using an analytical MSA 224S balance (Sartorius, Germany) and with a Density Determination Kit (Sartorius, Germany), followed by determining their apparent masses after immersion in water. The density was then determined using the following equation:

$$\rho = \left[\frac{W_{air}}{(W_{air} - W_{water})}\right] X\,(D_{water} - D_{air}) + D_{air} \quad (1)$$

where $\rho$ is the density of the specimen, $W_{air}$ is the mass of the specimen in air at 21 °C, $W_{water}$ is the mass of the specimen in water at 21 °C, $D_{water}$ is the density of water at 21 °C and $D_{air}$ is the density of air at 21 °C.

*2.2.2.4. Dynamic mechanical analysis (DMA).* The DMA 242C (Netzsch, Germany) was used to study the thermo-mechanical properties of the elastomers before and after hydrogen exposure, to estimate the possible changes as a result of hydrogen exposure. The tested samples had a dimension of (30 × 5*2) $mm^3$. The investigation was done using the 3-point bending mode under a constant frequency of 1 Hz and spanning a temperature range of −100 °C to +100 °C at 2 K/min. The results were evaluated from the plot of storage modulus ($E^{'}$), loss modulus ($E^{''}$), and loss factor (tan δ, $\frac{E^{''}}{E^{'}}$). The tan δ peak was used for the estimation of the glass transition temperature ($T_g$).

*2.2.2.5. Mechanical testing.* Mechanical properties under tensile loading were evaluated with a Zwick Universal testing machine (Zwick Roell, Germany) on dumbbell specimens (Type 2, ISO 37) to determine the influence of hydrogen exposure. Three specimens per elastomer were measured before, immediately after and 48 h after exposure according to the ISO-37 standard. The measurements were conducted with a testing speed of 500 mm/min and 50 mm clamping area. This test provided information on the tensile strength and modulus of elastomers after hydrogen exposure.

*2.2.2.6. Hardness measurement.* The hardness expressed in International Rubber Hardness Degrees (IRHD)-Normal tests were conducted via the Digi test IRHD-normal 30081.N (Zwick Roell, Germany) on three 10 × 10*2 $mm^3$ elastomer samples (stacked one on top of the other) before, immediately after and 48 h after hydrogen exposure to determine the hardness properties in hydrogen environment. The method N (normal test) is found appropriate for the determination of hardness in rubbers in the range 35 IRHD and 85 IRHD and therefore used for the elastomers in the study. The penetrating distance of the indenter and the magnitude of the indenting force are followed according to the ISO 48-2 Standard.

*2.2.2.7. Compression set.* The compression set was measured to determine the possible irreversible deformation resulting in the sample on the application of a compressive force at a fixed temperature. Two elastomer specimens from each type were tested before and two others after hydrogen exposure conditions. The tests were performed on cylindrical samples with a diameter of 13 mm and a thickness of 6 mm. Three 2 mm samples combined constituted one 6 mm sample required for this test. For the samples before exposure, the initial dimensions of the samples ($l_0$) were measured and then subjected to a 15 % deformation using a spacer bar of 5.6 mm, followed by transferring to an oven maintained at 100 °C for 24 h (ISO 815-1). The final thickness of the samples was measured after removing from the oven and cooling outside for 30 min.

The compression set is then calculated using the following equation:

$$\mathrm{CS}\ (\%) = \left[\frac{t_0 - t_1}{t_0 - t_n}\right] * 100 \quad (2)$$

where CS = compression set, $t_0$ = original height of the specimen, $t_1$ = final height of the specimen after 24 h of compression and 30 min of cooling at room temperature, $t_n$ = thickness of the spacer chamber (5.6 mm).

The specimens immediately after taking out from the hydrogen chamber are transferred to a temperature-controlled laboratory, where their thicknesses are measured until an equilibrium value has been

reached. This equilibrium value is noted as the original height of the specimen after exposure. Thereafter, the sample is inserted inside the spacer bar and the final dimension is recorded using the exact procedure as outlined in the ISO-815-1 standard.

*2.2.2.8. ATR FT-IR measurements.* The possible chemical changes in HNBR1 and HNBR2 were evaluated using Fourier transformed infrared spectroscopy (FT-IR). The ATR measurements of the spectra with the germanium crystal were carried out on the Hyperion 3000 (IR microscope) from Bruker. In each case 32 scans were measured at a resolution of 4 $cm^{-1}$. An atmospheric compensation, an extended ATR correction and a baseline correction were carried out for all spectra.

*2.2.2.9. Scanning electron microscopy measurements.* A scanning electron microscope, type EVO MA 10 (Carl Zeiss Microscopy GmbH, Jena, Germany) with a tungsten thermionic emitter was used for the morphological surface analysis of the HNBR2 rubber. The unexposed and exposed samples were coated with a layer of gold/palladium to improve the electrical conductivity of the sample. The micrographs were taken at an acceleration voltage of 10 kV and a secondary electron detector.

## 3. Results and discussion

### 3.1. Preliminary low-pressure hydrogen exposure tests

The preliminary tests conducted at low hydrogen pressures of 5 and 20 MPa at 120 °C yielded negligible changes with the two studied elastomers. The changes were low (approximately of 1 %) with a static exposure of 20 MPa and at 120 °C temperature. These results led to testing the samples at high pressure hence forming a focus area in this paper.

### 3.2. Static isobaric (100 MPa) and isothermal (120 °C) hydrogen exposure

#### 3.2.1. Appearance

The change in the visible specimen sizes immediately after taking out from the hydrogen chamber pointed to a swelling behavior after exposure to hydrogen gas up to 100 MPa. The exact dimensions of the samples along with their magnified images were measured using a powerful optical microscope. The optical images indicated the similar trend, confirming a swelling behavior from an increase in the dimensions of the samples (reflected by their percent increase in areas in Table 2). Under the high-pressure gas conditions, elastomers allow the gas diffusion into the component through the segmental mobility of the long polymer chains enabling easy saturation of the hydrogen gas in the void spaces of the polymer [18]. This dissolved gas upon depressurization, tends to expand, causing the elastomer to swell. The rapid decompression caused the hydrogen gas to come out of the polymer and create blisters on its surface (Fig. 3c and d). The blister formation was seemingly a temporary phenomenon and disappeared from the surface after several minutes of taking out from the chamber (up to 15 min), mostly in a continuous way. Some of them disappeared suddenly accompanied by a sound. At the end of this process no significant damage was observed at the surface of the specimen (Fig. 3e), but SEM images could detect some microcracks at the surface (Fig. 3g). It should be bear in mind that under operating conditions, the sealing materials is under mechanical compression, which should increase the risks of failure of the rubber materials, i.e. by extrusion or bending as described in Ref. [21].

**Table 2**
Summary of the physical properties' changes for the HNBR1 and HNBR2 elastomers when exposed to static high pressure up to 100 MPa and a temperature of 120 °C.

| Elastomer type | Physical properties | 7 days | | 21 days | |
|---|---|---|---|---|---|
| | % Change in properties after hydrogen exposure | Immediately after | 48hr after | Immediately after | 48hr after |
| HNBR1 | Mass | 0.63 % | −0.72 % | 0.64 % | −0.44 % |
| | Area | 15.1 % | −2.22 % | 14.8 % | −0.64 % |
| HNBR2 | Mass | 0.26 % | 0.04 % | 0.39 % | −0.12 % |
| | Area | 15.36 % | −1.96 % | 13.2 % | −0.59 % |

#### 3.2.2. Physical properties

The percent increase in area (change in dimensions of the samples confirmed by the panorama images of the samples) observed immediately after 7- and 21-days high-pressure hydrogen exposure also indicated the swelling phenomenon (Table 2). As expected, the percent increase in mass was found to be not as significant as that of the areas. Additionally, the changes occurring at 100 MPa pressure were around 10 times higher than that obtained by hydrogen pressures up to 20 MPa.

The density measurements and corresponding volume changes are illustrated in Fig. 4. Right after 7 days of exposure to hydrogen, the density of HNBR1 decreases by 15 % and the density of HNBR2 shows a reduction of about 18 % compared to their initial values. Similar behavior is found after 21 days of hydrogen exposure at 120 °C, as well as after 7 days under high pressure hydrogen at ambient temperature. On the other end, experiments performed at 120 °C and 0.1 MPa nitrogen environment did not lead to any density changes.

The corresponding volume increase is presented in Fig. 4b. This swelling behavior can be directly attributed to the diffusion of hydrogen through the polymer and rapid gas decompression. After 48 h, the volume reverted to its original values. The negative values after fully desorption of gas are probably due to migration of some additives in the materials as a result of high-pressure exposure.

Comparing the two materials, the volume increase reaches up to 20 % and 28 % immediately after 7 days of $H_2$ exposure for HNBR1 and HNBR2, respectively. Previous study performed after 24 h of high-pressure hydrogen exposure reported that the hydrogen uptake of NBR matrix increased with the carbon black filling ratio, but hydrogen adsorbed on carbon black did not contribute to the volume expansion [23]. This is in accordance with our results after 7 days and with 21 days of exposure, in which HNBR2 presents a higher volume increase given its lower carbon black content compared to HNBR1.

Further, as shown in Table 1, the mechanical properties of these two grades reveal that HNBR2 has higher hardness, higher tensile modulus compared with HNBR1. This in general would help to minimize the gas intake into the material. This would be in line with the lower mass increase in HNBR2. However, the higher CB loading of HNBR1 seemingly minimized the volume increase during decompression possibly due to gas adsorbed on the surface of the CB, additionally the high pressure might have originated microcracks inside the material, which would allow the released of gas and end up lowering the volume increase during decompression phase. In contrast, the gas in HNBR2 is dissolved mostly in the matrix or in PA-matrix interfaces. Despite lower mass increase of HNBR2, higher volume increase implies that the gas desorption from the material is significantly slow in HNBR2 compared with HNBR1 which is adversely effective to RGD properties.

The mass, area and density measurements of the elastomers reverted to their original values 48 h after taking out from the chamber, which indicated that the hydrogen exposure brought quasi no permanent change in the physical dimensions of the samples. But a slight reduction of mass may indicate the possible migration of certain additives due to

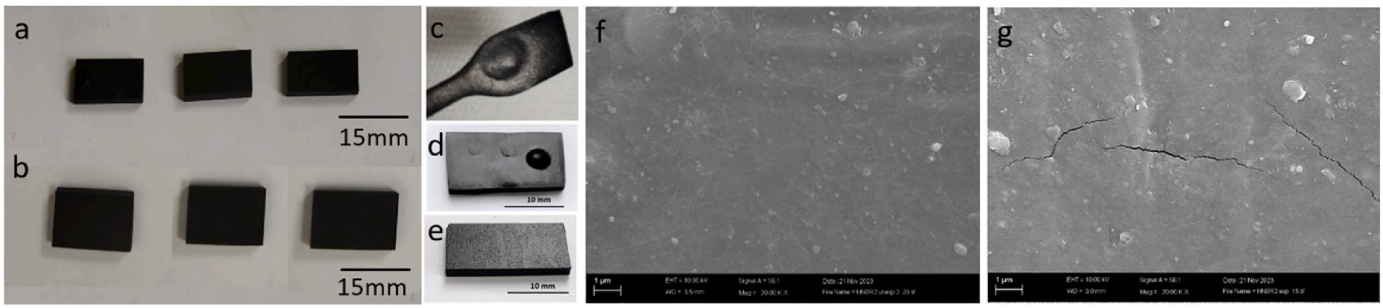


**Fig. 3.** Swelling behavior of HNBR1 samples observed, (a) before, and (b) immediately after high-pressure hydrogen exposure followed by blister formation after rapid release of pressure, (c) HNBR1 after immediately 21 days, (d) HNBR2 immediately after 7 days exposure, and (e) HNBR2 48 h after 7 days exposure; SEM images (f) HNBR2 before and (g) HNBR2 after 7 days exposure to hydrogen for 7 days, 100 MPa, 120 °C.

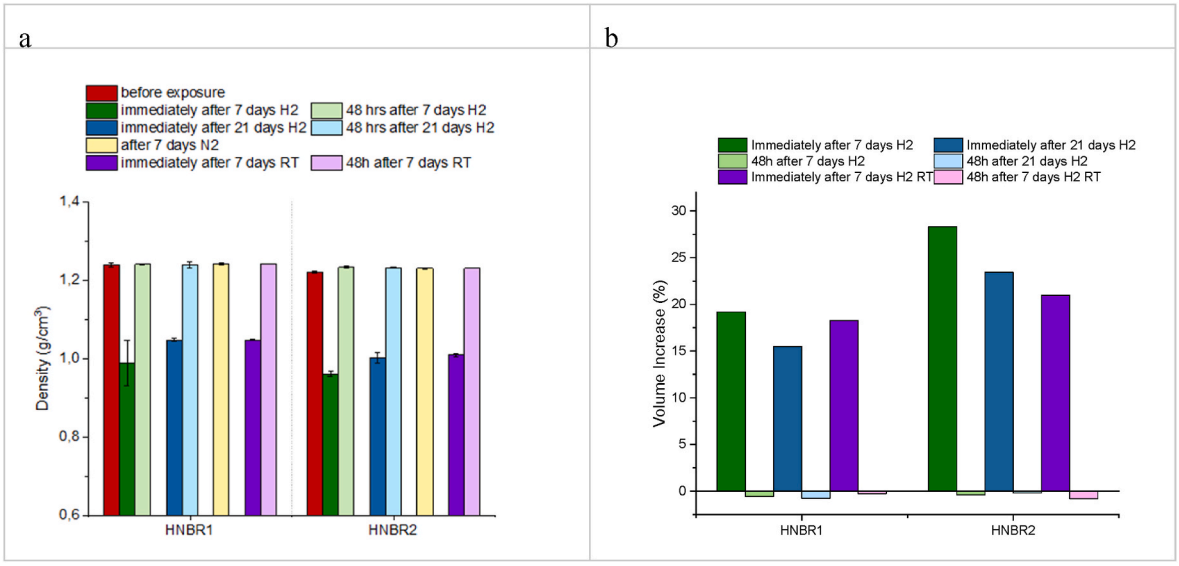


**Fig. 4.** a. Change in densities of the polymers HNBR1 and HNBR2 before, immediately after and 48 h after hydrogen exposure. The control experiments in nitrogen (yellow) indicate no change in densities in comparison to the density before exposure. b. Volume change of HNBR1 and HNBR2 before, immediately after and 48 h after hydrogen exposure (inverted bars). (For interpretation of the references to colour in this figure legend, the reader is referred to the Web version of this article.)

exposure to high-pressure hydrogen.

### 3.2.3. *Mechanical properties*

Dynamic mechanical properties of HNBR1 and HBNR2 were evaluated by DMA method. The storage moduli (E′), and loss factor (tan δ) peaks for the elastomers before and after high pressure hydrogen exposure are shown in Fig. 5. In the case of HNBR1, the storage modulus (see Fig. 5 a), seems unaffected at the glassy region for all exposure conditions, while at the rubbery plateau, HNBR1 shows an increase of the storage modulus (E′ at 25 °C) under the tested conditions. The effects of high temperature combined with high pressurized hydrogen atmosphere for 7 and 21 days, seem to be competitive. At high temperatures chain mobility is increased and more free volume is created, dissolved hydrogen can act as plasticizer and cause inflation of the polymer matrix resulting in an apparent looser network, this effect is dominant at least for the 7 days exposed sample. In the case of the HNBR1 sample exposed at 120 °C for 21 days, the stiffening effect is caused mostly by temperature and seems to be dominating over the softening caused by decompression. Exposure in nitrogen at 120 °C and 0.1 MPa during 7 days confirms the stiffening effect that temperature exerts in the material. An increase in the material's crosslink density is considered here unlikely since the temperature of exposure is too low to activate the peroxide curing agent if there is any remaining after the curing process.

Fig. 5 b shows the behavior of the Tanδ of HNBR1 for the different hydrogen exposure conditions and under high pressure hydrogen. HNBR1 shows a trend of decreasing $T_g$ values with the exposure conditions, although the difference is just around 2.5 °C degrees lower regard to its original $T_g$, this again, can be explained by the softening during decompression.

The storage modulus E′ of HNBR2 is shown in Fig. 5 c. The E′ of HNBR2 shows a slight increase in the glassy region, but a lower storage modulus in the rubbery plateau in all exposure conditions, except in the case of HNBR2 exposed at 120 °C under $N_2$ which shows a trend of increasing storage modulus and a similar stiffening of the matrix as seen in HNBR1. The samples exposed to high pressure $H_2$ show no significant changes after exposure regardless the time of exposure, this can be attributed to the reinforcing effect of PA fillers, as it will be discussed later, this stabilizing effect will be reflected as well in other mechanical properties such as tensile properties. The effect of hydrogen exposure on HNBR2 is barely perceptible with small changes of the $T_g$ of less than 1 °C, so the influence can be considered negligible.

The IRHD-Normal of the elastomers before, immediately after, 48 h after exposure and in nitrogen environment is shown in Fig. 6. Overall, the hydrogen retention in the polymer causes the elastomers to soften which was reflected in the decrease in the hardness values for both elastomers immediately after hydrogen exposure after 7 and 21 days. Comparing the unexposed materials, HNBR2 has a higher hardness, certainly due to its PA fillers. The HNBR1 elastomer, however, yielded a

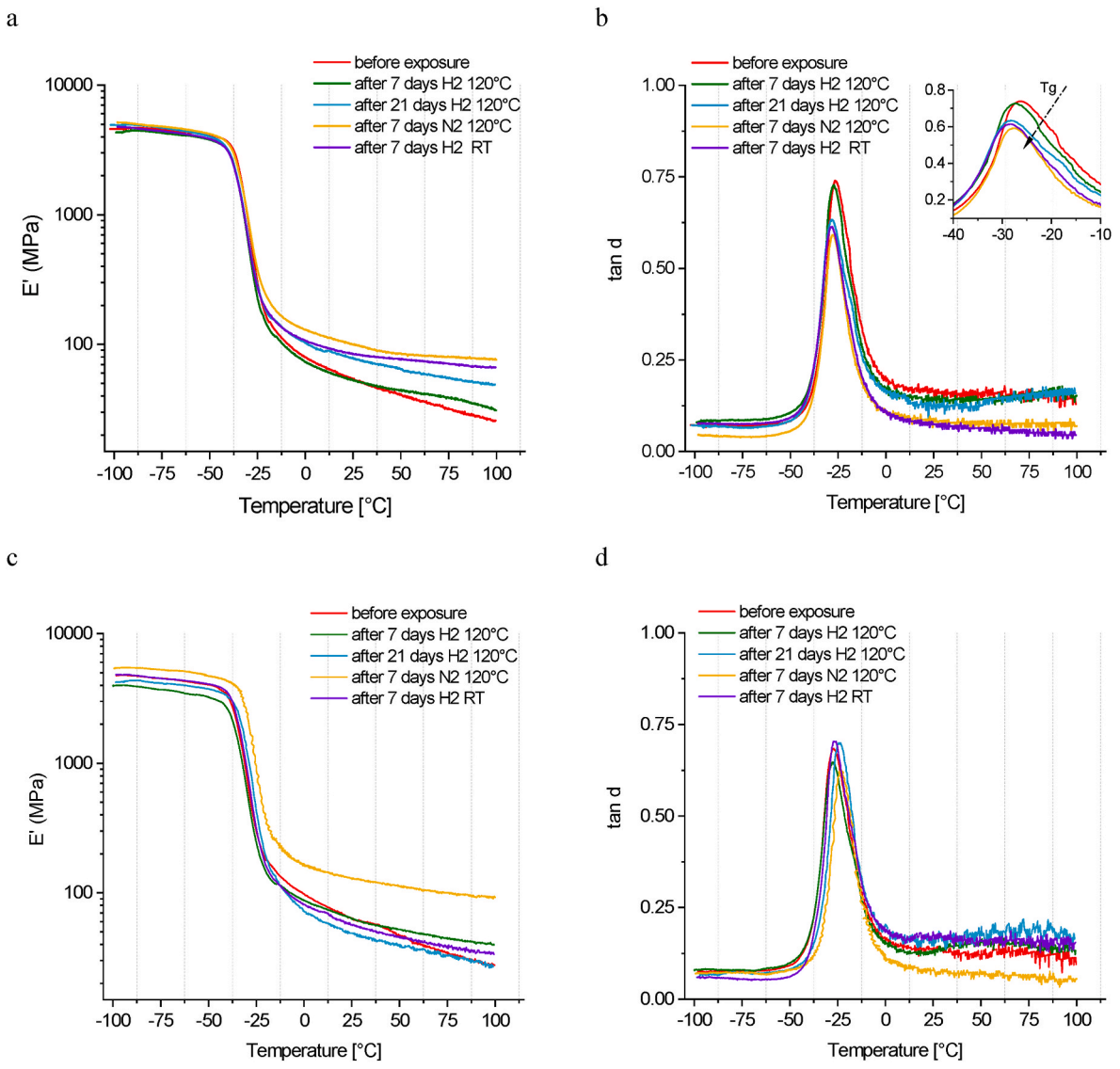


**Fig. 5.** a. Storage Modulus E′ of HNBR1. b. tanδ of HNBR1. The inset shows a slight shift of the glass transition temperature towards lower temperatures under the different exposure conditions. c. storage Modulus E′ of HNBR2 and d. tanδ of HNBR2.

slightly lower reduction in hardness (around 6 %) compared to the HNBR2 elastomers (around 7.5 %). 48 h after the specimens were taken out from the chamber, the samples showed hardness values very close to those of the unexposed materials, indicating that the hydrogen exposure causes no irreversible change in the hardness of the elastomers. The nitrogen exposed samples at 120 °C exhibited no change in hardness, in comparison to the samples before exposure, which explained the fact that the high-pressure hydrogen exposure was responsible for the change in hardness values.

The tensile properties in air were examined on dumbbell specimens of each of the two elastomers before and after 7- and 21-days exposure in high pressure hydrogen. The tensile stress-strain curves and characteristic values before and after hydrogen exposure are depicted in the supplementary material.

The tensile strength and elongation at break of the elastomers reduced significantly after hydrogen exposure, especially for HNBR1 (17 % and 14 % respectively) compared to HNBR2 (8 % and 10 % respectively). PA fillers may therefore be advantageous to improve the mechanical properties in high-pressure hydrogen condition, by reducing the gas intake in HNBR2. The effect of the exposure time is observed on the elongation at break but is minimal on the tensile strength for both elastomers. Additionally, the tensile strength returned to its original value 48 h after taking out from the hydrogen chamber after 7 days of exposure which indicated that there is no permanent loss of mechanical properties. The control experiments in nitrogen environment at 120 °C indicated almost no change in tensile properties in comparison to the properties before hydrogen exposure. This explained that the decrease in tensile strength could be related to the dissolution of high amount of hydrogen in the material, and that this deteriorates both the tensile strength and the elongation at break of filled NBR rubbers since hydrogen molecules dissolved in the rubber are mainly adsorbed at the interface between the matrix and fillers, impairing the reinforcing effect of the fillers [22].

Moreover, these results are in accordance with the earlier work carried out by Yamabe et al. [23], who studied the tensile strength of NBR rubbers exposed to hydrogen up to 100 MPa and 30 °C temperature. He found that the tensile elastic modulus decreased significantly with an increase in volume due to the softer material behavior due to $H_2$ in the material by swelling. This phenomenon is best explained by the following fitting formula [23]:

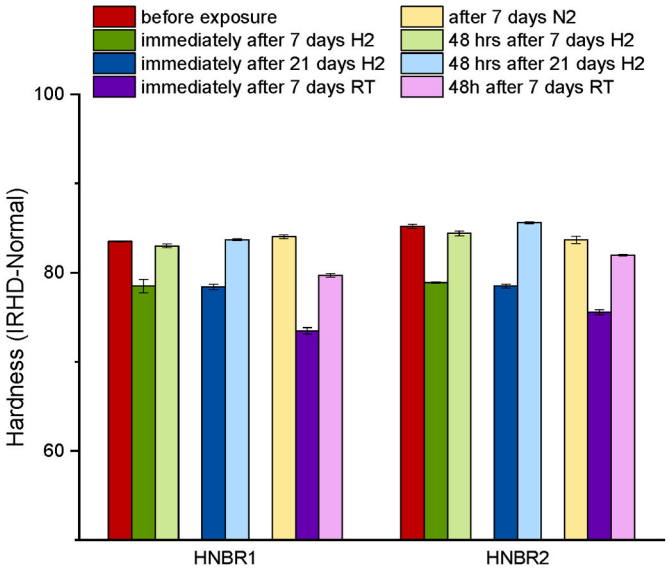


**Fig. 6.** Change in IRHD-Hardness of the polymers HNBR1 and HNBR2 before, immediately after and 48 h after hydrogen exposure. The control experiments in nitrogen indicate no change in hardness in comparison to the polymers before exposure.

$$E = E_0 \sqrt[3]{\left(\frac{V_0}{V}\right)} \tag{3}$$

where $E$ is the final elastic modulus, $E_0$ the initial elastic modulus, V the final volume and $V_0$ the initial volume of the sample. The latter is in agreement with our results, it is evident that the stress at break and the elongation at break are reduced after their exposure in hydrogen and measured immediately after (as seen in Fig. 7 a and b), for the sake of comparison, Table 3 shows the stress at 100 % of elongation or M100, there is a trend of decreasing modulus of the samples exposed to hydrogen at 120 °C as well as those exposed at room temperature compared to the samples measured 48 h later or exposed to high temperature but inert environment.

Compression set properties of HNBR1 and HNBR2 before and after hydrogen exposure are shown in Fig. 8. According to the results, both materials increased in compression set because of hydrogen exposure.

**Table 3**
Change in M100 modulus with experiment conditions.

| Condition | HNBR1 | HNBR2 |
|---|---|---|
| | M100 (MPa) | M100 (MPa) |
| Before Exposure | 17.1[a] | 19.9[a] |
| Immediately after 120 °C, 7 days in $H_2$ | 16.2 | 18.9 |
| 48 h after 120 °C, 7 days in $H_2$ | 17.5 | 20.3 |
| Immediately after RT, 7 days in $H_2$ | 16.5 | 19.2 |
| After 120 °C, 7 days in N2 | 17.4 | 21 |
| Immediately after 120 °C, 21 days in $H_2$ | 16.9 | 19.5 |
| After 120 °C, 7 days in $N_2$ | 17.4 | 21 |

[a] Measured in our labs after conditioning but before exposure.

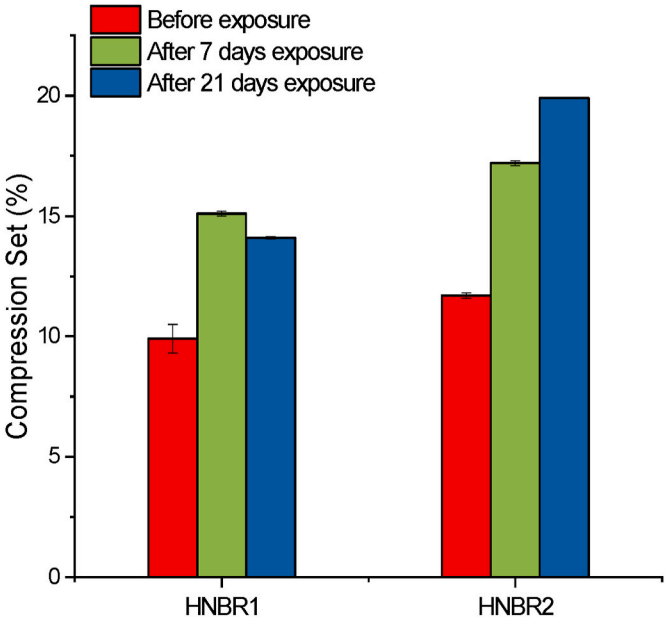


**Fig. 8.** Plot showing the compression set properties of HNBR1 and HNBR2 before, after 7 days and after 21 days exposure.

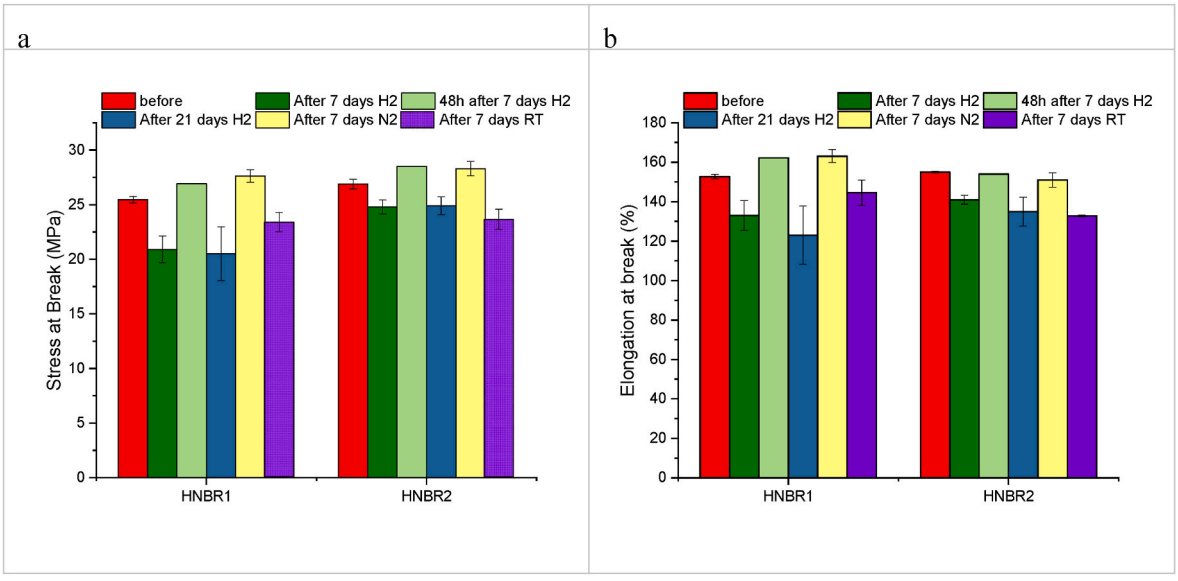


**Fig. 7.** Tensile properties of HNBR1 and HNBR2 before and immediately after hydrogen or nitrogen exposure.

This increase after hydrogen exposure might suggest therefore a permanent chemical or physical deformation in the elastomers as result of the exposure experiments.

Comparing the grades, HNBR2 has a higher compression set after 21 days. Lu et al. [24] reported an inverse relation of the compression set with increase in the filler content, which couldn't be verified in this study. It would be expected that the lower carbon black content and additionally PA fillers in HNBR2 grades would contribute to reduce the compression set.

As observed previously for NBR materials after hydrogen exposure, the compression set is greatly affected by addition of fillers and plasticizers. Hydrogen that diffused into the polymer acts as a solvent and thereby increase the mobility of fillers to promote aggregation. In his recent study, Simmons found a significant morphological changes in the plasticizer-incorporating rubber after exposure which could be related to potential chemical change in the materials [9]. In this experiment, a possible migration of the fillers is also suggested, as seen later with the AFM analyses.

### 3.2.4. Surface analyses

Fig. 9 shows the absorption spectrum of HNBR1 before, after 7 days and after 21 days of exposure to hydrogen at 120 °C and 100 MPa. The characteristic peaks of the HNBR and CB are distinguishable and exhibit very small shifts in their characteristic absorption peaks. Nevertheless, some subtle changes in the intensities of the absorption in the samples can be noticed. A shoulder at 2960 $cm^{-1}$ disappears after the hydrogen exposure, this peak is related to the C–H stretching of functional groups bonded to aromatic cycles and located at the surface of CB particles and/or aggregates in the polymer matrix [25]. An increase in the intensity of the 1730 $cm^{-1}$ peak is also detected, as well as a small increase around the 1538 $cm^{-1}$ peak and 877 $cm^{-1}$ corresponding to the C═C bonds in the aromatic cycles of CB, since the intensity of the IR absorption is an indication of the concentration of the infrared absorbers, then it is possible that the high-pressure exposure caused additives to be pushed away as well as migration/aggregation of CB networks towards the rubber surface after the decompression and hydrogen desorption. Regard to the characteristic peaks of HNBR, it is accurate to state that no further hydrogenation took place as result of the hydrogen exposure by the absence of any absorption between 3400 and 3300 $cm^{-1}$. It is noteworthy however, the appearance and increase of intensity of the 1538 $cm^{-1}$ band after 21 days of hydrogen exposure at 120 °C, this peak is directly related to the presence of carbon black, as in this case

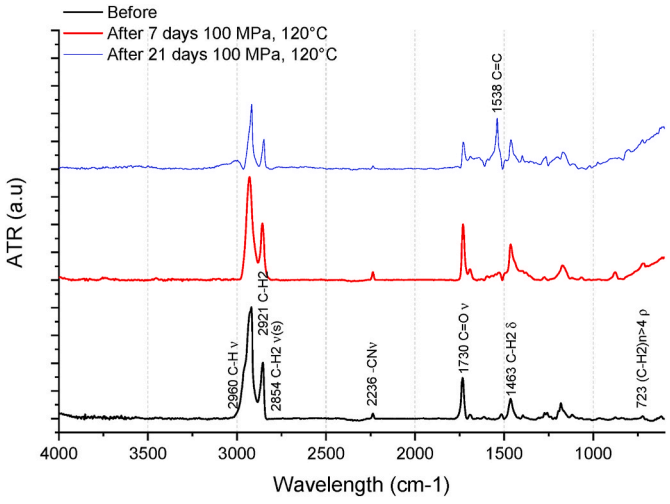


**Fig. 9.** FT-IR Spectra of HNBR1 before and after hydrogen exposure at 120 °C and 100 MPa for 7 days and after 21 days. The spectrum has been normalized to 2854 $cm^{-1}$ which corresponds to the symmetric stretching of the $C–H_2$ functional groups in HNBR.

FT-IR-ATR is a spectroscopic method with a low depth of incidence, the absorption is associated only with the sample surface.

Topographic scans of the HNBR1 grade after 7 days of hydrogen exposure at high pressure and 120 °C using AFM in tapping mode, show a change in the surface as can be seen in Fig. 10b compared to the initial surface appearance as shown in Fig. 10a.

Before the hydrogen exposure, the sample surface showed characteristic scratches from its compounding, still smooth areas are distinguishable, and the brighter higher areas correspond to CB. After the exposure, the surface evolves towards an apparent more intricated morphology with small vesicles or folds, a smaller and more abundant domains of carbon black can be noticed appearing closer to the surface of the polymer matrix, this was a feature of some regions of the sample, smooth regions were also present after the exposure. However, the roughness values calculated from these AFM images yielded 67.576 nm as the roughness value from the sample before exposure, and for the sample after exposure the value is 38.100 nm, as if after exposure the sample surface has been inflated and appeared softer or smoother in average.

Phase images (see Fig. 10b.) reveal the presence of the carbon black particles within the vesicular regions, since the particles are stiffer and have a smaller adhesion with the AFM tip, the phase shift is smaller, as can be seen in Fig. 10b. The areas with exposed carbon black particles match the spectroscopic analysis, since the particles domain are pushed towards the surface because of the high hydrogen pressure and high temperature, a higher absorption corresponding to the CB particles should be detected. Similarly, these more exposed particles might be responsible for the reduction of intensity of loss factor, a subtle hardening as seen in the rubbery plateau in the storage modulus E' and, also the subtle decrease of the hardness when compared to the HNBR2 grade.

Measurements of roughness performed with Nanofocus (Fig. SM5) comprising a larger area of the material account for very slight decrease in roughness after the exposure, from 4 roughness profiles of 4.8 mm length each the average roughness value for the samples before exposure is 2.002 μm and for the sample after the exposure the value is 1860 μm.

An evaluation of possible chemical changes in HNBR2 was conducted through FT-IR-ATR (Fig. 11), in this case the characteristic peaks of the HNBR2 show a very subtle shift. Nevertheless, the intensities of the peaks are increasing with the hydrogen exposure and temperature as it is expected from a temperature aged polymer. In both rubber grades the 1730 peak and 1538 peak are increasing, however it is important to keep in mind that these peaks are possibly associated to CB. After 21 days of exposure of the HNBR2 grade, a dramatic increase of the 1538 $cm^{-1}$ band, as in case of HNBR1, is not detected, presumably because of its lower CB content. Nevertheless, a small peak at 3297 $cm^{-1}$, could be attributed to the stretching vibration of N–H in PA, as well as the increase in the 1647 $cm^{-1}$ is due to C═O stretching (Amide I). This could be associated to an increased amount of the PA fillers present on the sample surface, particularly in the HNBR2 sample after 7 days of exposure at 120 °C. Scanning electron microscopy and AFM topographic and phase images were used to inspect the change of the sample surface morphology before and after the hydrogen exposure.

As shown in the SEM images in Fig. 3, an apparent smoother surface with some features (denser regions) are distinguishable, after hydrogen exposure, these features become more evident, as well as cracks that have been developed after the exposure.

The topographic scans on the HNBR2 sample, before and after exposure to hydrogen for 7 days, 100 MPa, 120 °C, are shown in Fig. 12. The globular structures detected in the sample before exposure appear to be more abundant on the surface of the sample after exposure, and some of the features are more protuberant. These are related to CB aggregates present on the surface just as in the case of HNBR1. The phase image before exposure needs to be analysed in relation to a previous characterization of the HNBR-PA composite by M. Hemstede-van Urk et al., the AFM characterization of the PA dispersion in HNBR (10 phr) can be found in reference [19]. The phase image in Fig. 12c before the exposure

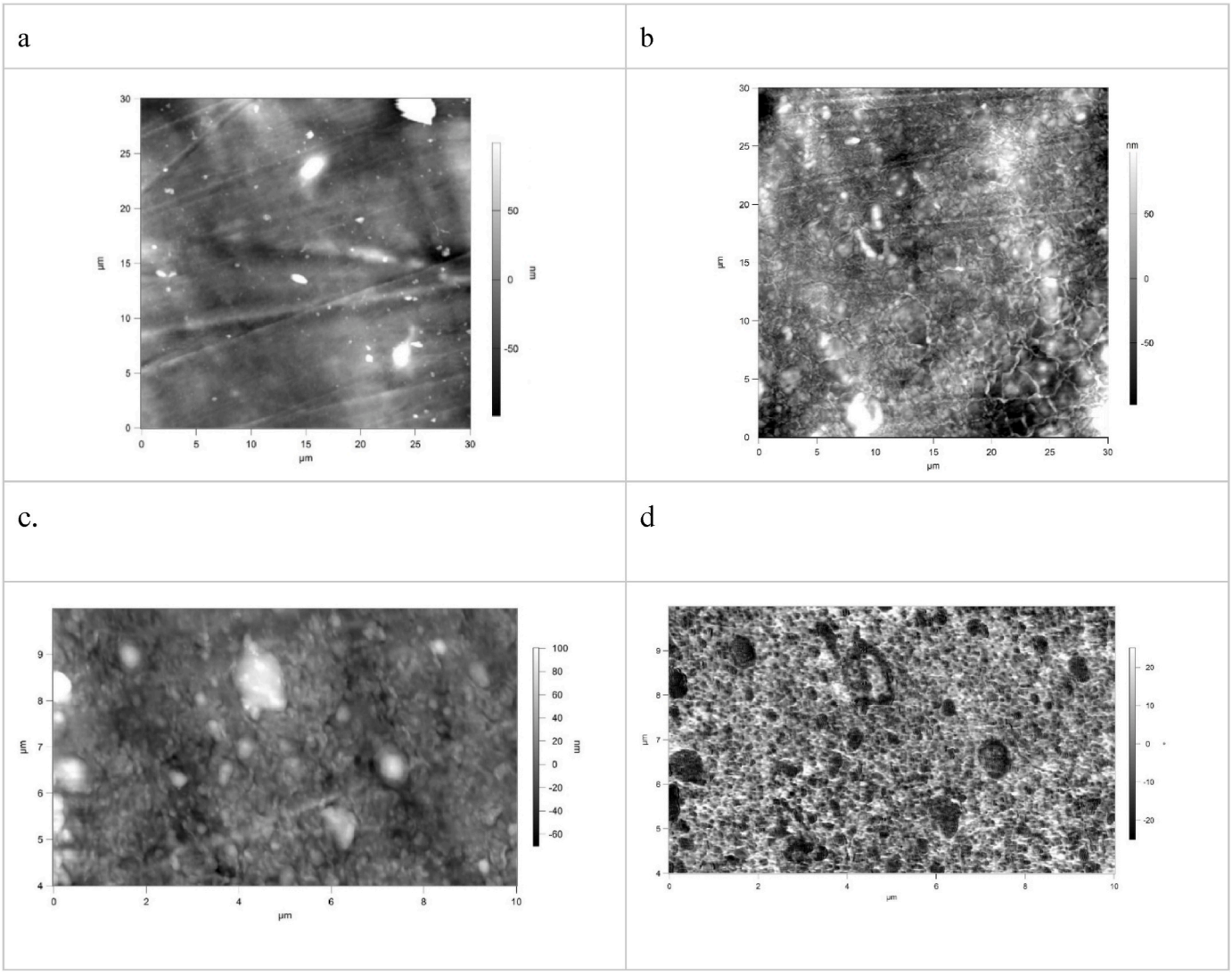


**Fig. 10.** AFM tapping mode topography scans of HNBR1 a. before and b. after 7 days in hydrogen at 120 °C, c. Topographic scan of a region with vesicles and exposed CB particles, d. Phase image, the areas with less adhesion are shown darker, in this case, related to CB particles.

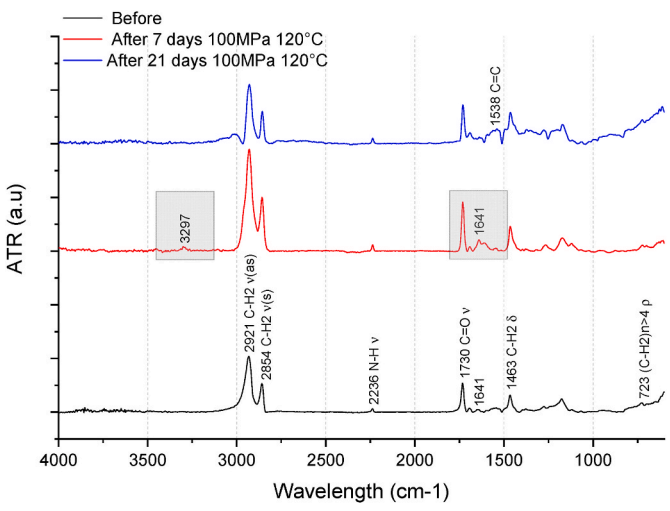


**Fig. 11.** FT-IR Spectra of HNBR2 before and after hydrogen exposure at 120 °C and 100 MPa for 7 days and after 21 days. The spectrum has been normalized to 2854 $cm^{-1}$ which corresponds to the symmetric stretching of the C–$H_2$ functional groups in HNBR.

shows a softer matrix (higher phase shift) and darker spots (in phase) the latter with sizes ranging from 0.6µm to 1.4 µm, these as compared to Ref. [19] are assigned to PA domains in the rubbery matrix. After $H_2$ exposure (Fig. 12d), these domains appear to be wider and more abundant on the surface. The features corresponding PA appear to blend and yield bigger areas in phase with the tapping frequency (darker areas), this is also in agreement with the appearance of characteristic PA IR absorption bands, from this it is inferred that PA fillers and CB could have pushed out by the decompression and promote crack formation on the material surface.

## 4. Conclusion

With the increasing demand in material testing in hydrogen, new test facilities are now available at BAM. This study presents the influence of high-pressure hydrogen environment on the physical and mechanical properties of two types of cross-linked hydrogenated acrylonitrile butadiene rubbers. Following the methodology of the CSA/ANSI Standard, characterization of the material properties was performed before and after static exposure experiments in hydrogen up to 100 MPa at 120 °C for 7 and 21 days.

Overall, the effect of high-pressure exposure on these two materials led to swelling with formation of blisters and microcracks due to rapid

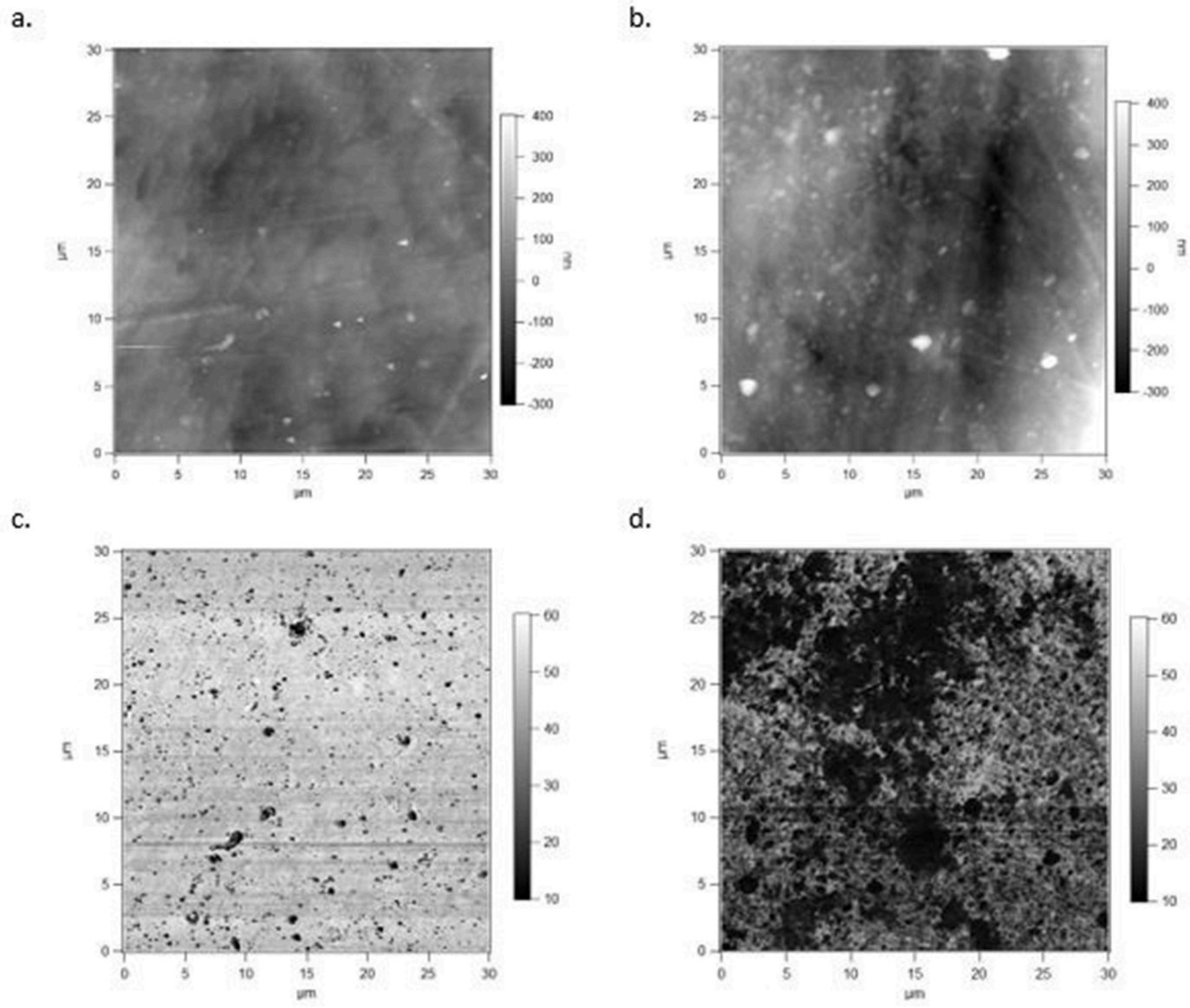


**Fig. 12.** AFM topography images of the surface of HNBR2 a. before and b. after exposure to hydrogen for 7 days, 100 MPa, 120 °C and AFM phase images of the surface of HNBR2 c. before and d. after exposure to hydrogen for 7 days, 100 MPa, 120 °C.

decompression. Decreased density and mechanical properties were observed on both rubbers immediately after exposure but recovered to their original values after 48 h. The addition of PA fillers in CB filled HNBR had a beneficial effect on the mechanical properties of the rubber in hydrogen. After hydrogen exposure, CB domains were exposed towards the surface, as it was possible to confirm by AFM and FT-IR Spectroscopy. DMA results didn't show a clear trend possible due to competitive phenomenon taking place under these testing conditions, for example, hardening of materials and softening due to hydrogen dissolution and plasticization. Therefore, a further study will be necessary to understand the respective aspects.

As these grades were especially developed for high-pressure gas conditions, they show relatively high resistance to damage under these conditions. However, in operating conditions, the sealing materials is under mechanical compression, which should increase the risks of failure of the rubber materials. Based on this methodology, new materials developed within this framework will be characterized. Furthermore, tribological and mechanical experiments in situ are being made and will be the focus of the next publication.

## Declaration of competing interest

The authors declare that they have no known competing financial interests or personal relationships that could have appeared to influence the work reported in this paper.

## Acknowledgment

The authors would like to thank M. Schulze, M. Reimer, Ms. Fengler and M. Opitz for performing the physical and mechanical tests, Ms. Hidde for the FT-IR collection, and Ms. Weimann for the electron microscopy characterization as well as M. Askar for organizing the hydrogen exposure. A particular thank goes to Brunero Cappella for the AFM measurements and to Ms. C. Neumann and Ms. N. Slachciak for the roughness measurements.

The research work was performed within the COMET-project "Polymers4Hydrogen" (project-no.: 21647053) at the Bundesanstalt für Materialforschung und -prüfung (BAM) within the framework of the COMET-program of the Federal Ministry for Climate, Action, Environment, Energy, Mobility, Innovation and Technology and the Federal

Ministry for Digital and Economic Affairs with contributions by Polymer Competence Center Leoben GmbH (PCCL, Austria), Montanuniversität Leoben (Department Polymer Engineering and Science, Chair of Chemistry of Polymeric Materials, Chair of Materials Science and Testing of Polymers), Technical University of Munich, Tampere University of Technology, Politecnico di Milano and Arlanxeo Deutschland GmbH, ContiTech Rubber Industrial Kft., Peak Technology GmbH, SKF Sealing Solutions Austria GmbH, and Faurecia.

## Appendix A. Supplementary data

Supplementary data to this article can be found online at https://doi.org/10.1016/j.ijhydene.2024.01.148.

## References

[1] Balasooriya W, et al. A review on applicability, limitations, and improvements of polymeric materials in high-pressure hydrogen gas atmospheres. Polym Rev 2021:1–36.
[2] Schlapbach L, Züttel A. Hydrogen-storage materials for mobile applications. Materials for sustainable energy: a collection of peer-reviewed research and review articles from nature publishing group. 2011. p. 265–70.
[3] Eberle U, Müller B, Von Helmolt R. Fuel cell electric vehicles and hydrogen infrastructure: status 2012. Energy Environ Sci 2012;5(10):8780–98.
[4] Sgobbi A, et al. How far away is hydrogen? Its role in the medium and long-term decarbonisation of the European energy system. Int J Hydrogen Energy 2016;41(1):19–35.
[5] Zhang F, et al. The survey of key technologies in hydrogen energy storage. Int J Hydrogen Energy 2016;41(33):14535–52.
[6] Barthélémy H, Weber M, Barbier F. Hydrogen storage: recent improvements and industrial perspectives. Int J Hydrogen Energy 2017;42(11):7254–62.
[7] Amirante R, et al. Overview on recent developments in energy storage: mechanical, electrochemical and hydrogen technologies. Energy Convers Manag 2017;132:372–87.
[8] Zheng Y, et al. A review on effect of hydrogen on rubber seals used in the high-pressure hydrogen infrastructure. Int J Hydrogen Energy 2020;45(43):23721–38.
[9] Simmons KL, et al. H-Mat hydrogen compatibility of polymers and elastomers. Int J Hydrogen Energy 2021;46(23):12300–10.
[10] Ono H, Fujiwara H, Nishimura S. Penetrated hydrogen content and volume inflation in unfilled NBR exposed to high-pressure hydrogen–What are the characteristics of unfilled-NBR dominating them? Int J Hydrogen Energy 2018;43(39):18392–402.
[11] Nishimura S. Rubbers and elastomers for high-pressure hydrogen seal. Kobunshi 2015;64(6):356–7.
[12] Nishimura S, Fujiwara H. Detection of hydrogen dissolved in acrylonitrile butadiene rubber by 1H nuclear magnetic resonance. Chem Phys Lett 2012;522:43–5.
[13] Yamabe J, Nishimura S, Koga A. A study on sealing behavior of rubber O-ring in high pressure hydrogen gas. SAE International Journal of Materials and Manufacturing 2009;2(1):452–60.
[14] Yamabe J, Nishimura S. Influence of fillers on hydrogen penetration properties and blister fracture of rubber composites for O-ring exposed to high-pressure hydrogen gas. Int J Hydrogen Energy 2009;34(4):1977–89.
[15] Fujiwara H, Ono H, Nishimura S. Degradation behavior of acrylonitrile butadiene rubber after cyclic high-pressure hydrogen exposure. Int J Hydrogen Energy 2015;40(4):2025–34.
[16] Zhou C, et al. Sealing performance analysis of rubber O-ring in high-pressure gaseous hydrogen based on finite element method. Int J Hydrogen Energy 2017;42(16):11996–2004.
[17] Zhou C, Chen G, Liu P. Finite element analysis of sealing performance of rubber D-ring seal in high-pressure hydrogen storage vessel. J Fail Anal Prev 2018;18(4):846–55.
[18] Menon NC, et al. Behaviour of polymers in high pressure environments as applicable to the hydrogen infrastructure. In: Pressure vessels and piping conference. American Society of Mechanical Engineers; 2016.
[19] Hemstede-van Urk M, , et alTherban HT. Polyamide reinforced HNBR with improved high temperature properties. In: Rubberworld; 2020. p. 1741. Akron Peninsula Rd. Akron, OH 44313 USA.
[20] Association CS. CSA/ANSI CHMC 2:19. Test methods for evaluating material compatibility in compressed hydrogen applications — polymers. CSA Group; 2019.
[21] Koga A, Uchida K, Yamabe J. Evaluation on high-pressure hydrogen decompression failure of rubber O-ring using design of experiments. International Journal of Automotive Engineering 2011;2:123–9.
[22] Jeon SK, et al. Relationships between properties and rapid gas decompression (RGD) resistance of various filled nitrile butadiene rubber vulcanizates under high-pressure hydrogen. Mater Today Commun 2022;30.
[23] Yamabe J, Nishimura S. Tensile properties and swelling behavior of sealing rubber materials exposed to high-pressure hydrogen gas. Journal of Solid Mechanics and Materials Engineering 2012;6(6):466–77.
[24] Lu Y, et al. Effect of filler on the compression set, compression stress–strain behavior, and mechanical properties of polysulfide sealants. J Appl Polym Sci 2011;120(4):2001–7.
[25] Ferraro G, et al. Multiscale characterization of some commercial carbon blacks and diesel engine soot. Energy Fuels 2016;30(11):9859–66.